The effects of vitamin D deficiency on cerebral circulation

PhD thesis

Éva Pál PharmD

Doctoral School of Theoretical and Translational Medicine
Semmelweis University

Supervisors: Zoltán Benyó, MD, PhD, DSc
Szabolcs Várbíró, MD, PhD, Med. Habil.

Official reviewers: Sándor Nardai, MD, PhD
Ferenc Domoki, MD, PhD

Head of the Complex Examination Committee:
Gábor Varga, MD, PhD, DSc

Members of the Complex Examination Committee:
Barna Vásárhelyi, MD, PhD, DSc
Csaba Ambrus, MD, PhD

Budapest
2020

1. Introduction

Vitamin D (VitD) is a lipid-soluble vitamin that functions as a steroid hormone. Its biological actions are mediated mainly by the VitD receptor (VDR), which belongs to the nuclear receptor superfamily. VitD controls the expression of more than 200 genes, thereby it participates in the modulation of several physiological functions. Accordingly, vitamin D deficiency (VDD) has been linked to several disorders including cardiovascular diseases. The cardiovascular effects of VitD include the modulation of immune, inflammatory and endothelial functions. Furthermore, VitD regulates cell proliferation and migration, renin expression and extracellular matrix homeostasis; it mediates vascular growth and angiogenesis, it stimulates nitric oxide production and inhibits the generation of reactive oxygen species.

Ischemic stroke belongs to the leading causes of death and disability worldwide. However, cerebral circulation has a well-developed defense system to protect the brain from ischemia including large vessels of the Willis circle and smaller pial anastomoses between the terminal branches of cerebral arteries which may compensate for the occlusion of a cerebral artery. Although VDD appears to increase the risk and severity of ischemic stroke, the impact of VitD on the cerebrovascular system is still unclear.

According to the literature, androgen excess is likely to increase the incidence of cerebrovascular diseases. Interestingly, 67–85% of women with androgen excess are also affected by VDD. In addition, VDD may worsen the cardiovascular manifestation of hyperandrogenic disorders. Although both VDD and hyperandrogenism appear to be associated with cerebrovascular disorders, their combined effect on cerebral arteries has not been examined before.

2. Objectives

Although VDD has been associated with increased risk and severity of cerebrovascular diseases including ischemic stroke, the impact of VitD on the cerebrovascular system and thus, on cerebrovascular adaptation to ischemia has not been examined before. Furthermore, the increased incidence of cerebrovascular disorders in men and in hyperandrogenic women as compared to premenopausal healthy women has been proven by several studies; however, the role of testosterone in the cerebrovascular manifestation of VDD has not been revealed previously.

In our experiments, we aimed at investigating:

- the impact of VDD on the morphological, biomechanical and functional properties of cerebral arteries,
- the interplay between testosterone and VDD in the remodeling of cerebral arteries,
- the role of vitamin D signaling in cerebrovascular adaptation to unilateral carotid artery occlusion, laying emphasis on the pial collateral circulation.

3. Methods

Animals

Male and female, four-week-old Wistar rats were either fed with VitD deficient diet (VitD content less than 5 IU/kg) for eight weeks **(VDD** and ♀***D-*** groups) or received conventional rat chow with per os VitD (20.000 IU/mL cholecalciferol) supplementation (daily VitD intake: 300 IU/100 g b. w.) providing optimal VitD supply (**Control** and ♀***D+*** groups). Half of the female rats from both groups received transdermal testosterone treatment (0.033 mg/g b. w.) for eight weeks (***T*♀*D+*** and ***T*♀*D-*** groups). Another set of experiments was performed on adult (103 (98–122) days) male mice carrying a mutant, functionally inactive vitamin D receptor (**VDR$^{\Delta/\Delta}$**) and their wild-type (**WT**) littermates on C57BL/6 genetic background. The experiments were carried out according to the guidelines of the Hungarian Law of Animal Protection (XXVIII/1998) and were reported in compliance with the ARRIVE guidelines. All procedures were approved by the National Scientific Ethical Committee on Animal Experimentation.

Pressure microangiometry

Anterior cerebral artery (ACA) segments were isolated and excised from rat brains, and their morphological and functional properties were examined using pressure microangiometry. After equilibration (30 min, 50 mmHg intraluminal pressure in normal Krebs-Ringer solution bubbled with a gas mixture (5% CO_2, 20% O_2, 75% N_2) at 37°C), 10^{-4} mol/L uridine-5'-triphosphate (UTP) was added to the chamber followed by the administration of 10^{-6} mol/L bradykinin. Finally, the organ chamber was filled with Ca^{2+}-free Krebs solution and after 20

min the pressure was increased from 0 to 150 mmHg in 10 mmHg steps. Pictures were taken during the experiment by a digital camera connected to an inverted microscope. The outer and inner diameters of the vessels were measured by ImageJ image analysis software.

Histology and immunohistochemistry

ACA segments were freshly fixed with formalin for histological examination and stained with Weigert's resorcin-fuchsin, hematoxylin and eosin, and immunostained for smooth muscle actin, androgen receptor (AR), endothelial nitric oxide synthase (eNOS), and cyclooxygenase-2 (COX-2). Data collections were made by microscope coupled with video-camera. Pictures were analyzed with ImageJ image analysis software (except for resorcin-fuchsin staining, which was evaluated with Leica Qwin software). Optical density of the endothelial layer after eNOS and COX-2 staining, the percentage of positively stained tissue area to total area of the sections after AR staining, and the nucleus count of tunica media were determined.

***In vivo* cerebrocortical blood flow measurement using laser-speckle imaging**

Mice were anesthetized with isoflurane (2%) during femoral artery cannulation and with intraperitoneally applied ketamine (100 μg/g b. w.) and xylazine (10 μg/g b. w.) throughout the rest of the experiment. Following femoral artery and trachea cannulation, a loose knot was placed around the left common carotid artery for the later induction of carotid artery occlusion (CAO). Thereafter, the head of the mouse was secured in a stereotaxic head holder, and the skull was exposed by retracting the scalp following a midline incision. The cerebrocortical blood flow (CoBF) was measured using laser-speckle imaging. First,

atipamezole (1 μg/g ip.) was administered to reverse xylazine's α-2-agonistic effects, then 10 min were allowed to acquire baseline data of CoBF and blood pressure. Thereafter, the left common carotid artery was occluded by tightening the loose knot around the vessel. The average baseline CoBF for 1 min preceding CAO was determined as a reference value (100%), and changes in CoBF until 5 min after CAO were recorded and expressed as a percentage of the reference CoBF. The area between the CoBF curves (ABC) of the hemispheres ipsilateral and contralateral to CAO was determined for each animal. The first 30 sec after CAO was considered as the acute phase, and the following 270 sec as the subacute phase of adaptation. CoBF changes were measured in four predefined and standardized cortical regions of interest: frontal, parietal, temporal cortices, and the zone of pial anastomoses of both hemispheres. The body temperature of mice was maintained between 37 and 38 °C throughout the experiments. Systemic arterial pressure was measured continuously using the left femoral artery cannula, whereas oxygen saturation, heart rate, and respiratory rate were determined using a pulse oximeter on the depilated right hindlimb. At the end of each experiment, the femoral artery cannula was used for arterial blood sampling in order to determine arterial blood gas tensions, acid/base parameters, and plasma ion concentrations. The physiological parameters of mice (weight of body, heart, left ventricle, and brain, length of tibia) were also measured.

Evaluation of the morphology of pial collaterals

For visualization of the cerebrocortical vasculature, mice were perfused transcardially with 10 mL heparinized (10 IU/mL) saline solution followed by the injection of 2 mL mixture of black inks into the left cardiac ventricle under isoflurane (2%) anesthesia. Thereafter, the brains were removed

and immersed in 4% formaldehyde solution. Pictures of the dorsal surface of the brain were taken with a digital camera connected to a microscope. The morphological analysis of the leptomeningeal collaterals connecting the branches of the ACA and the middle cerebral artery (MCA) was performed using ImageJ software. The number and the tortuosity index (the ratio of vessel curve length over the line distance between the two ends of the vessel) of the collaterals were determined, and the anastomotic points were identified as the half distance between the nearest branching points of the ACA and the MCA branches. Adjacent anastomotic points were connected by the anastomotic line, and the distance between the anastomotic line and the midline at 4 mm caudally from the frontal pole of the brain (level of bregma) was measured.

Data analysis

The normal distribution of datasets was checked with the Shapiro–Wilk test. If the normal distribution was verified, data were presented as the arithmetic mean and standard error, and p-values were determined by Student's unpaired t-test or by two-way ANOVA followed by the appropriate post hoc test. If data were not normally distributed, they were presented as the median and interquartile range, for which the Mann–Whitney test was used to determine statistical significance. Statistical analysis and graph plotting were performed with GraphPad Prism software and $p<0.05$ was considered as a statistically significant difference.

4. Results

4.1. VDD-induced alterations of cerebral arteries in male rats

4.1.1. Physiological parameters of rats

VDD did not influence the physiological parameters (body weight, heart/body weight, testis weight, mean arterial blood pressure, heart rate) and serum hormone levels (testosterone, androstenedione, progesterone) of rats. However, the VitD-deficient diet supported significantly lower serum 25-hydroxyvitamin D levels.

4.1.2. Cerebral arterial morphology

In spite of the well-preserved systemic cardiovascular and metabolic parameters, VDD induced marked changes in the morphology and reactivity of cerebral arteries. VDD increased wall thickness and the wall thickness/lumen diameter ratio (Figure 1A, **$p<0.01$, two-way repeated measures ANOVA followed by Bonferroni post hoc test, n=10-11). In addition, the wall cross-sectional area increased significantly in VDD as compared to the Control group (Figure 1B, *$p<0.05$, Student's unpaired t-test, n=9-9). VDD increased the thickness of the tunica media but it did not affect the thickness of the tunica intima. Additionally, significantly increased nucleus counts were found in the smooth muscle layer of arteries from the VDD group (Figure 1C, ****$p<0.0001$, Student's unpaired t-test, n=4-6). These alterations imply the presence of hypertrophic remodeling in VDD.

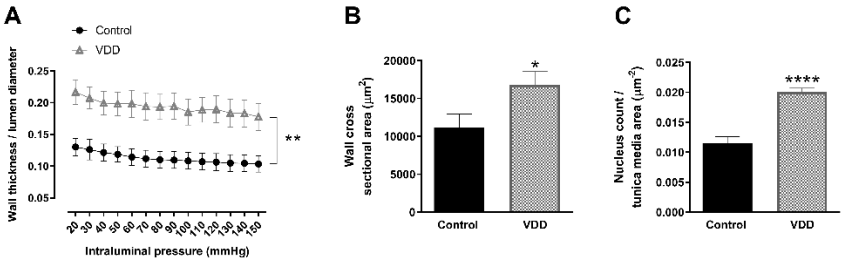

Figure 1. Remodeling of the arterial wall in VDD.

4.1.3. Biomechanical properties

In accordance with the increased wall-to-lumen ratio, the tangential wall stress was significantly lower in the VDD group under passive conditions. However, the elastic modulus, distensibility, and the density of the elastic fibers did not differ between the groups.

4.1.4. Immunohistochemistry

The optical density of endothelial eNOS staining was lower in the VDD group, indicating lower expression of eNOS. In contrast, COX-2 expression was enhanced in the endothelial layer of arteries from the VDD group. The percentage of positively stained area following AR staining, therefore the expression of AR protein in the vessel wall was decreased in VDD as compared to control animals.

4.1.5. Smooth muscle tone and endothelial reactivity

Bradykinin induced slight vasodilatation after precontraction in the Control group, but it failed to relax the arteries from the VDD group (Figure 2A, *$p<0.05$, Student's unpaired t-test, n=9-9), indicating endothelial dysfunction in VDD. The myogenic

tone (Figure 2B, **p<0.01, Student's unpaired t-test, n=8-8) as well as the UTP-induced contraction (Figure 2C, *p<0.05, Student's unpaired t-test, n=10-9) increased in VDD.

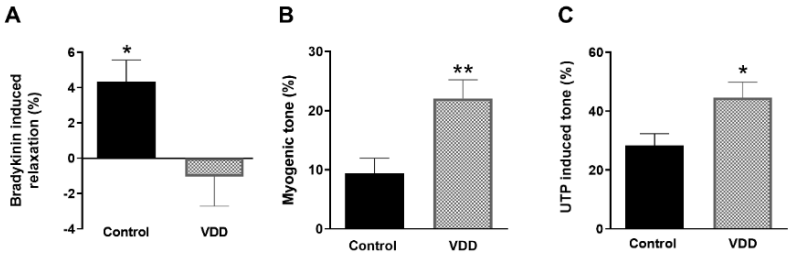

Figure 2. Alterations of vascular reactivity induced by VDD.

4.2. Role of hyperandrogenism in the cerebrovascular manifestation of VDD in female rats

Neither VDD nor androgen excess caused any changes in the wall thickness of female rats. Surprisingly, however, combined VDD and hyperandrogenism significantly increased the wall thickness (Figure 3A, *p<0.05 vs. ♀*D*+, two-way ANOVA followed by Tukey's post hoc test, n=5-7). In accordance with these findings, the lumen cross sectional area was only decreased by combined VDD and androgen excess (Figure 3B, *p<0.05 vs. ♀*D*+, #p<0.05 vs. *T*♀*D*+, two-way ANOVA followed by Tukey's post hoc test, n=10-11), indicating that VDD results in increased active tension and/or inward remodeling in the presence of testosterone.

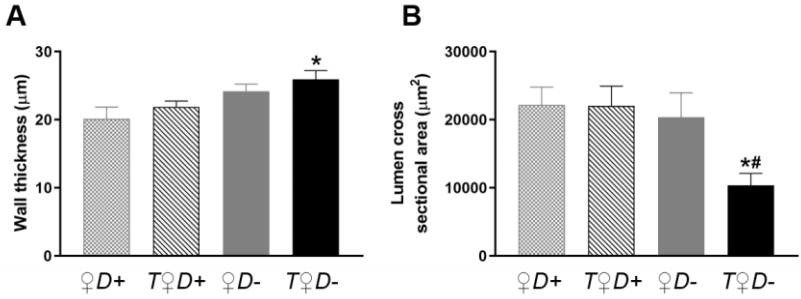

Figure 3. Cerebrovascular remodeling in combined VDD and hyperandrogenism.

4.3. Effects of VDR deficiency on the cerebrovascular adaptation to unilateral CAO

4.3.1. Physiological parameters of mice

The physiological parameters (heart weight, heart weight/body weight ratio, left ventricle weight, brain weight, heart rate, respiratory rate, plasma ion concentrations) of male $VDR^{\Delta/\Delta}$ mice did not differ from the WT littermates, except for body weight and tibial length (both parameters decreased in $VDR^{\Delta/\Delta}$ mice). Neither blood pressure nor arterial blood gas parameters (partial pressures of carbon dioxide and oxygen, oxygen saturation) were impacted by ablation of VitD signaling.

4.3.2. Regional cerebrocortical blood flow changes after CAO

In the frontal region ipsilateral to CAO neither WT nor $VDR^{\Delta/\Delta}$ mice showed significant CoBF reduction after CAO as compared to the contralateral side, and similar results were obtained in the parietal region of WT animals. On the contrary, in the parietal region of $VDR^{\Delta/\Delta}$ mice, CoBF was reduced

significantly in the acute phase after CAO and normalized thereafter. More pronounced changes were observed in the temporal region: CAO resulted in pronounced but transient hypoperfusion in the ipsilateral temporal cortex in WT animals, whereas CoBF remained significantly reduced during the whole measurement in $VDR^{\Delta/\Delta}$ mice (Figure 4, *p<0.05, **p<0.01, ***p<0.001, ****p<0.0001, two-way repeated measures ANOVA followed by Bonferroni post hoc test, n=8-8). In the zone of pial anastomoses, both WT and $VDR^{\Delta/\Delta}$ mice showed transient hypoperfusion in the ipsilateral hemisphere as compared to the contralateral side, although CoBF recovered much later in $VDR^{\Delta/\Delta}$ than WT animals.

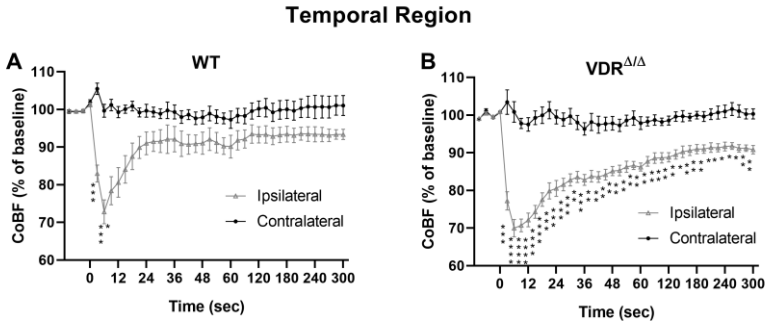

Figure 4. CoBF changes of the temporal region in WT and $VDR^{\Delta/\Delta}$ mice following CAO.

In order to pinpoint the direct effect of CAO unmasked by CoBF alterations related to potential fluctuations of systemic physiological parameters (e.g. arterial blood pressure or blood gas values), we determined the area between the CoBF curves (ABC) of the hemispheres ipsilateral and contralateral to CAO for each mouse. Furthermore, we differentiated between the acute (0-30 sec after CAO) and subacute (30-300 sec after CAO) phases of CoBF changes. Functional VDR inactivity caused a

more pronounced decrease of CoBF in the parietal region and in the zone of pial anastomoses in the acute phase, indicating an impaired cerebral vasoregulation, whereas during the subacute phase this difference disappeared. In contrast, VDR inactivity resulted in increased ABC (i.e. decreased CoBF in the ipsilateral temporal cortex) both in the acute (Figure 5A, *p<0.05, Student's unpaired t-test, n=8-8) and in the subacute phase (Figure 5B, *p<0.05, Mann-Whitney test, n=8-8,), indicating a more severe vasoregulatory dysfunction in the temporal cortex of $VDR^{\Delta/\Delta}$ mice. Neither blood pressure nor oxygen saturation were impacted by ablation of VitD signaling, therefore we could exclude the possibility that any differences in systemic arterial blood pressure or in arterial blood gas tensions would influence the CoBF changes after CAO.

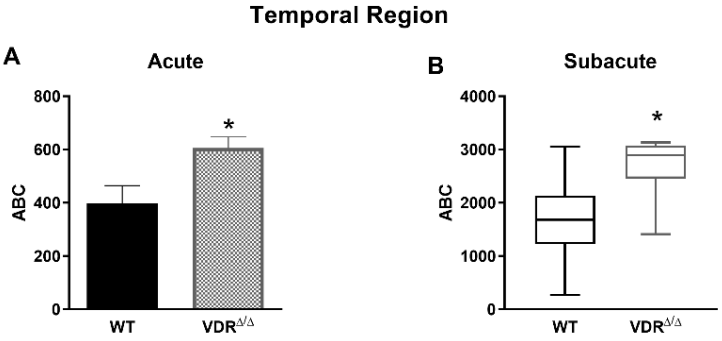

Figure 5. Differences in CoBF changes in the temporal region induced by CAO in $VDR^{\Delta/\Delta}$ vs. WT mice in the acute and the subacute phases of adaptation.

4.3.3. Effects of VDR deficiency on the intracranial collateral circulation

Ablation of VitD signaling caused a reduction in the number of pial MCA-to-ACA collaterals, and an increased tortuosity of these collateral vessels (Figure 6A,C; *p<0.05, **p<0.001, Student's unpaired t-test, n=6-6), indicating an impaired development of leptomeningeal anastomoses. In addition, the anastomotic line was closer to the midline in $VDR^{\Delta/\Delta}$ mice as compared to WT animals (Figure 6B, *p<0.05, Mann–Whitney test, n=6-6), indicating that the territory supplied by the MCA was increased at the expense of the territory of ACA. All these alterations have a negative impact on the capacity of leptomeningeal collaterals to compensate the consequences of CAO and can explain the more pronounced drop and delayed recovery of CoBF in the temporal cortex of $VDR^{\Delta/\Delta}$ mice.

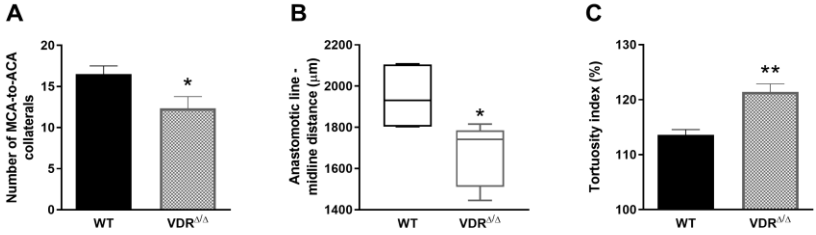

Figure 6. Morphological alterations in the pial collaterals of VDD mice.

5. Conclusions

In our experiments, we aimed at investigating the impacts of vitamin D deficiency on the morphological and functional characteristics of cerebral circulation. Our results indicate that:

- Vitamin D deficiency induces hypertrophic remodeling *via* enhanced vascular smooth muscle cell proliferation in cerebral arteries of male rats.
- Vitamin D deficiency causes an increase in vessel tone and a decrease in endothelial relaxation capacity accompanied by enhanced COX-2 and decreased eNOS and AR protein expression in cerebral arteries.
- In female rats, vitamin D deficiency combined with androgen excess leads to vascular remodeling in cerebral arteries. Cerebrovascular manifestation of vitamin D deficiency requires androgen excess and depends on gender, implying an interplay between androgens and vitamin D in the cerebral circulation.
- Ablation of vitamin D signaling compromises the cerebrovascular adaptation to unilateral carotid artery occlusion in male mice characterized by reduced cerebrocortical blood flow in the parietal and temporal regions of the ipsilateral hemisphere.
- The highest vulnerability of the temporal cortex of vitamin D receptor deficient mice, indicated by the most pronounced drop and delayed recovery of the blood flow following carotid artery occlusion can be attributed to the impaired development of leptomeningeal anastomoses characterized by decreased number, increased tortuosity and altered location of collaterals between the middle and anterior cerebral arteries.

6. Bibliography of the candidate's publications

Publications related to the dissertation

Pál É, Hricisák L, Lékai Á, Nagy D, Fülöp Á, Erben RG, Várbíró S, Sándor P, Benyó Z. Ablation of Vitamin D Signaling Compromises Cerebrovascular Adaptation to Carotid Artery Occlusion in Mice. Cells. 2020; 12;9(6):E1457. **IF: 4.366**

Pál É*, Hadjadj L*, Fontányi Z, Monori-Kiss A, Lippai N, Horváth EM, Magyar A, Horváth E, Monos E, Nádasy GL, Benyó Z, Várbíró S. Gender, hyperandrogenism and vitamin D deficiency related functional and morphological alterations of rat cerebral arteries. PLoS One. 2019; 13;14(5):e0216951.
Contributed equally to this work.* **IF: 2.740

Pál É, Hadjadj L, Fontányi Z, Monori-Kiss A, Mezei Z, Lippai N, Magyar A, Heinzlmann A, Karvaly G, Monos E, Nádasy G, Benyó Z, Várbíró S. Vitamin D deficiency causes inward hypertrophic remodeling and alters vascular reactivity of rat cerebral arterioles. PLoS One. 2018; 6;13(2):e0192480.
IF: 2.776

Publications not related to the dissertation

Sziva RE, Fontányi Z, **Pál É**, Hadjadj L, Monori-Kiss A, Horváth EM, Benkő R, Magyar A, Heinzlmann A, Benyó Z, Nádasy GL, Várbíró S. Vitamin D Deficiency Induces Elevated Oxidative and Biomechanical Damage in Coronary Arterioles in Male Rats. Antioxidants (Basel). 2020; 9(10): 997. **IF: 5.014**

Hinsenkamp A, Ézsiás B, **Pál É**, Hricisák L, Fülöp Á, Besztercei B, Somkuti, Smeller L, Pinke B, Kardos D, Simon M, Lacza Z, Hornyák I. Crosslinked hyaluronic acid gels with blood-derived protein components for soft tissue regeneration. Tissue Eng Part A. 2020 Sep 29. **IF: 3.496**

Török M, Horváth EM, Monori-Kiss A, **Pál É**, Gerszi D, Merkely P, Sayour AA, Mátyás C, Oláh A, Radovits T, Merkely B, Ács N, Nádasy GL, Várbíró S. Chronic swimming training resulted in more relaxed coronary arterioles in male and enhanced vasoconstrictor ability in female rats. J Sports Med Phys Fitness. 2020 Jul 30. **IF: 1.432**

Török M, Monori-Kiss A, **Pál É**, Horváth E, Jósvai A, Merkely P, Barta BA, Mátyás C, Oláh A, Radovits T, Merkely B, Ács N, Nádasy GL, Várbíró S. Long-term exercise results in morphological and biomechanical changes in coronary resistance arterioles in male and female rats. Biol Sex Differ. 2020; 12;11(1):7. **IF: 3.267**

Hadjadj L, **Pál É**, Monori-Kiss A, Sziva RE, Korsós-Novák Á, Horváth EM, Benkő R, Magyar A, Magyar P, Benyó Z, Nádasy GL, Várbíró S. Vitamin D deficiency and androgen excess result eutrophic remodeling and reduced myogenic adaptation in small cerebral arterioles in female rats. Gynecol Endocrinol. 2019; 35(6):529-534. **IF: 1.571**

Hadjadj L, Monori-Kiss A, Horváth EM, Heinzlmann A, Magyar A, Sziva RE, Miklós Z, **Pál É**, Gál J, Szabó I, Benyó Z, Nádasy GL, Várbíró S. Geometric, elastic and contractile-relaxation changes in coronary arterioles induced by Vitamin D deficiency in normal and hyperandrogenic female rats. Microvasc Res. 2019; 122:78-84. **IF: 2.730**

Hadjadj L, Várbíró S, Horváth EM, Monori-Kiss A, **Pál É**, Karvaly GB, Heinzlmann A, Magyar A, Szabó I, Sziva RE, Benyó Z, Buday M, Nádasy GL. Insulin resistance in an animal model of polycystic ovary disease is aggravated by vitamin D deficiency: Vascular consequences. Diab Vasc Dis Res. 2018;15(4):294-301. **IF: 2.357**

Cumulative impact factor: **29.749**